HHS Public Access

Author manuscript

J Neuroimmune Pharmacol. Author manuscript; available in PMC 2019 June 01.

Published in final edited form as:

J Neuroimmune Pharmacol. 2018 June ; 13(2): 204–218. doi:10.1007/s11481-017-9775-0.

FDC:TFH Interactions Within Cervical Lymph Nodes of SIV-infected Rhesus Macaques

Rajnish S. Dave[1,*], **Ravi K. Sharma**[2,3,*], **Roshell R. Muir**[4], **Elias Haddad**[4], **Sanjeev Gumber**[5], **Francois Villinger**[6], **Artinder P. Nehra**[2], **Zafar K. Khan**[2], **Brian Wigdahl**[2], **Aftab A. Ansari**[4], **Siddappa N. Byrareddy**[1,†], and **Pooja Jain**[2,†]

[1]Department of Pharmacology and Experimental Neuroscience, University of Nebraska Medical Center, Omaha, NE USA

[2]Department of Microbiology and Immunology, and the Institute for Molecular Medicine and Infectious Disease, Drexel University College of Medicine, Philadelphia, PA USA

[3]Advanced Eye Center, Post Graduate Institute of Medical Education and Research, Chandigarh, India

[4]Division of Infectious Disease and HIV Medicine, Department of Medicine, Drexel University College of Medicine, Philadelphia, PA USA

[5]Department of Pathology & Laboratory Medicine, School of Medicine and Emory Vaccine Center, Emory University, Atlanta, GA USA

[6]New Iberia Research Center, University of Louisiana at Lafayette, New Iberia, LA USA

Abstract

Cerebrospinal fluid (CSF) drains via the lymphatic drainage pathway. This lymphatic pathway connects the central nervous system (CNS) to the cervical lymph node (CLN). As the CSF drains to CLN via the dural and nasal lymphatics, T cells and antigen presenting cells pass along the channels from the subarachnoid space through the cribriform plate. Human immunodeficiency virus (HIV) may also egress from the CNS along this pathway. As a result, HIV egressing from the CNS may accumulate within the CLN. Towards this objective, we analyzed CLNs isolated from rhesus macaques that were chronically-infected with simian immunodeficiency virus (SIV). We detected significant accumulation of SIV within the CLNs. SIV virion trapping was observed on follicular dendritic cells (FDCs) localized within the follicular regions of CLNs. In addition, SIV antigens formed immune complexes when FDCs interacted with B cells within the germinal centers. Subsequent interaction of these B cells with CD4+ T follicular helper cells (T_{FHs}) resulted in infection of the latter. Of note, 73% to 90% of the T_{FHs} cells within CLNs were positive for SIV p27 antigen. As such, it appears that not only do the FDCs retain SIV they also transmit them (via

[†]Address for correspondence: 2900 Queen Lane, Suite G47A, Philadelphia, PA 19129 USA. Tel: (215) 991-8393, Fax: (215) 848-2271, pjain@drexelmed.edu; sid.byrareddy@unmc.edu.

[*]Equal contribution

Compliance with Ethical Standards: This article does not contain any studies with human participants performed by any of the authors. All applicable international, national, and/or institutional guidelines for the care and use of animals were followed. For the detailed ethical statement please refer to materials and methods.

Conflict-of-interest disclosure: The authors declare no competing financial interests

B cells) to T_{FHs} within these CLNs. This interaction results in infection of T_{FHs} in the CLNs. Based on these observations, we infer that FDCs within the CLNs have a novel role in SIV entrapment with implications for viral trafficking.

INTRODUCTION

Influx of HIV into the central nervous system (CNS) begins early during infection, long before symptoms of neuroAIDS arise (1), via infected cells or free virus particles that cross the blood brain barrier (BBB) (2). Eventually, HIV reservoirs are established in cells or tissues that harbor replication-competent virus for prolonged periods of time. The viral reservoir is an archive of viral sequences representative of earlier stages of infection (3–5). Both HIV patients and simian immunodeficiency virus (SIV)-infected rhesus macaques (RMs) exhibit persistently high levels of viral DNA positive cells, with profound immune activation during combination antiretroviral therapy (cART) (6, 7). Despite effective cART, HIV viral reservoirs persist and represent a major roadblock of antiviral therapy interruption strategies and HIV cure strategies. The resident CNS cells like, perivascular macrophages and glial cells have been thought to be potent reservoir sites for HIV infection, thereby limiting the success of cART in completely suppressing viral replication within the CNS (8–10). The viral gene flow between the meninges and deep brain tissues was also reported upon HIV-1 infection (11).

Functional meningeal lymphatic system facilitates the drainage of the cerebrospinal fluid (CSF) to the cervical lymph nodes (CLNs) (12–18). This system also allows immune cells to migrate from cribriform plate into the lymphatic system of nasal mucosa and then into deep cervical lymph nodes (CLNs) (14). This meningeal lymphatic system creates a direct link to deep CLNs enabling drainage of CSF and immune cells egressing from the CNS (14, 15). CLNs constitute a cluster of numerous lymph nodes found in the collar region. These CLNs are a major site for systemic activation of CNS specific T cells, after presentation of antigen entrapped in dendritic cells (DCs) (19, 20). CNS-derived antigens have been shown to induce immune responses in the deep CLNs (21). Circulating conventional DCs (cDCs) had been shown to migrate through the rostral migratory stream (RMS) toward the olfactory bulb draining into CLNs (15). In this respect, we and others have clearly established trafficking of cDCs into the CNS in response to neuroinflammation (3, 4, 22–27). More recently, we have provided evidence for the presence of cDCs in the brain parenchyma of SIV-infected RMs (28).

In periphery, cDCs carrying HIV migrate into peripheral lymph nodes where they infect and prime T cells in the T-cell zone, which then move toward the B-cell follicles (BCFs). These BCFs harbor a specialized type of dendritic cell population designated follicular dendritic cells (FDCs) (29, 30), which can bind and retain antigen on their dendritic processes for months to years in the form of immune complexes (31, 32). BCFs have been postulated as important compartments for both latent and active viral reservoirs during treatment (33). In HIV disease, virion-immune complexes get trapped on the processes of FDCs, which interconnect to form a dense meshwork and represent the largest repository of virus in the body for longer time periods (3, 5, 31, 34). FDCs have recently been shown to retain

infectious HIV inside endosomes, indicating the migration of virions across these cells (35). Interestingly, FDCs have been shown to retain infectious HIV particles even in the presence of neutralizing antibodies, and infectious virus has been rescued from FDCs from HIV-infected patients on suppressive cART for up to 24 years, suggesting that FDCs represent a significant reservoir of diverse HIV (5, 35–39). Furthermore, even with suppressive antiretroviral therapy, replicating virus can persist to replenish FDC network (40). A similar pathway might exist for HIV antigens and HIV-infected cells from CNS to CLNs that are particularly important in the context of CNS related immune responses. Understanding viral distribution within the CLNs may shed new light on HIV infection of the CNS. The present study is the first attempt in this direction providing clear evidence for the abundance of SIV virions within FDCs' network of deep CLNs.

MATERIALS AND METHODS

Animals and Samples

A total of 11 SIV infected adult Indian rhesus macaques along with a naïve control animal were utilized in this study. All animals were maintained at the Yerkes National Primate Research Center of Emory University (Atlanta GA) in accordance with the regulations of the Committee on the Care and Use of Laboratory Animal Resources. All experiments were approved by the local institutional biosafety review and animal use and care committees. Rhesus macaques were inoculated intravenously with 200 $TCID_{50}$ (50% tissue culture infective dose) of SIVmac251. Peripheral blood samples were obtained concurrent with the times of biopsy samples. Peripheral blood mononuclear cells (PBMCs) were isolated from blood of SIV infected rhesus macaques, using standard Ficoll-Hypaque gradient procedure. Plasma viral RNA (vRNA) loads were measured in the corresponding blood samples. CLNs and other tissues were collected immediately after euthanasia from all animals for *in situ* techniques and flow cytometry analysis. Tissues were fixed by immersion in freshly prepared 4% paraformaldehyde and embedded in paraffin. To collect CLN cells, tissue was minced and sieved through 40-μm nylon cell strainers (Fisher Scientific, Pittsburgh, PA) with a 10 ml syringe plunger.

Ethics Statement

All animals were born and maintained at the Yerkes National Primate Research Center of Emory University in accordance with the rules and regulations of the Committee on the Care and Use of Laboratory Animal Resources, and according to the guidelines of the Committee on the Care and Use of Laboratory Animals of the Institute of Laboratory Animal Resources, National Research Council and the Department of Health and Human Services guidelines titled *Guide for the Care and Use of Laboratory Animals*. The animals were fed a monkey diet (Purina, Wilkes-Barre PA) supplemented daily with fresh fruits or vegetables and water *ad libitum*. Additional social enrichment, including the delivery of appropriate safe toys, was provided and overseen by the Yerkes enrichment staff. Animal health was monitored daily and recorded by the animal care staff and veterinary personnel, available 24 hours a day and 7 days a week. Monkeys were caged in socially compatible same-sex pairs to facilitate their well-being and social enhancement. Monkeys showing signs of sustained weight loss, disease, or distress were subject to clinical diagnosis based on symptoms and

then provided standard dietary supplementation, analgesics, and/or chemotherapy. The Yerkes National Primate Research Center has been fully accredited by the Association for Assessment and Accreditation of Laboratory Animal Care International.

Necropsy

Animals showing signs of clinical end points relative to disease progression were humanely euthanized with an intravenous overdose of pentobarbital sodium according to the guidelines of the American Veterinary Medical Association. A complete necropsy was performed on these animals. For histopathology or immunohistochemical examination, selected tissue samples were fixed overnight in 4% paraformaldehyde, embedded in paraffin and sectioned at 4 μm.

Quantitative RT-PCR and Quantitation of SIV RNA in plasma

Plasma and tissue RNA was isolated using the QiaAmp vRNA Mini-procedure and RNeasy Mini procedure, respectively, as described by the manufacturer (Qiagen, Germantown MD). vRNA levels were measured by quantitative RT-PCR (qRT-PCR) as described previously. The assay sensitivity was 50 vRNA copies per ml for plasma. RNA copy numbers in tissues were normalized and represented as SIV RNA copies per ng of total RNA (41).

Immunohistochemistry

Immunohistochemistry (IHC) was performed using 4μm thick, formalin fixed, FFPE tissue sections. Slides were baked, deparaffinized in xylene, and passed through a series of increasing percentage of alcohols. Subsequently, antigen was retrieved with 10 mM citrate buffer, pH 6.0 in a water bath warmed to 95°C for 1 hour. Slides were cooled to room temperature for 20 minutes and washed three times for 5 min with phosphate buffered saline (PBS) containing 0.05% Tween 20. Subsequently, slides were incubated for 30 min in PBS containing 0.1% Triton X-100. Slides were blocked with 10% normal goat serum (Jackson ImmunoResearch, West Grove PA) and subsequently incubated with 1:50 dilution of anti-CD35 and SIV gag (p27) monoclonal antibody (clone 55-2F12) in PBS overnight at 4°C. Slides were washed three times in PBS containing 0.025% Triton X-100, and treated with HRP-conjugated Goat anti-mouse (Novus Biologicals, Littleton CO) for 1 hour at room temperature. After further washing, immunoperoxidase staining was developed using DAB chromogen procedure as described by the manufacturer (Biocare Medical, Concord CA) for 10 min. Slides were counterstained with hematoxylin and mounted with permount aqueous mounting medium.

Immunofluorescence staining and quantitative image analysis

Immunofluorescence (IF) staining and quantitative image analysis was performed with frozen CLN sections of 4–5 μm thickness. Tissue Sections were baked overnight on glass slides at 55°C to firmly affix and dehydrate the tissue. Paraffin-embedded rhesus macaque CLN tissue sections were deparaffinized in xylene and rehydrated in a graded series of alcohol. Briefly, slides were immersed twice in 100% xylene for 3 min followed by a 3 min wash with a 1:1 solution of xylene and 100% ethanol. Subsequently, tissue sections were washed in 100, 95, 70 and 50% ethanol followed by a cold-water bath, each for 3 min.

Thereafter, tissue sections were boiled in 10 mM sodium citrate, pH 6.0 for 20 min, followed by three 5 min washes with PBS containing 0.05% Tween 20. For p27 and PD-1 staining, tissue sections were permeabilized in 0.1% triton X-100. Tissue sections were blocked with the Sniper reagent (Biocare, Concord CA) for 15 min. After blocking, tissue sections were stained with unconjugated primary mouse anti-human CD35 (clone E11; Novus Biologicals, Littleton CO), rabbit anti-human CD20 (polyclonal, Thermo Scientific, Rockford IL), goat anti human PD-1 (C-16, Santa Cruz Biotech, Dallas TX), mouse anti-p27 SIV gag (clone 55-2F12, AIDS Research and Reference Reagent Program, Germantown MD) or fluorescein peanut agglutinin (PNA) (Vector Labs, Burlingame CA) at a dilution ranging from 1:20 to 1:100 in PBS containing 1% BSA and incubated overnight at 4°C. Thereafter, tissue sections were washed and incubated with secondary fluorophore conjugated antibodies (TRITC-conjugated donkey anti-mouse, DyLight405-conjugated donkey anti-rabbit, DyLight405 conjugated donkey anti-goat or FITC-conjugated goat anti-mouse antibodies; Jackson Labs, West Groove PA) at a dilution ranging from 1:100–1:500 in PBS containing 1% BSA for 1 hour at room temperature. Since anti-CD35 and anti-p27 antibodies were generated in mouse, tissue sections were blocked after first primary antibody with 10% normal mouse serum followed by incubation with Fab fragment donkey anti-mouse (Jackson ImmunoResearch, West Groove PA) for 1 hour at room temperature. Subsequently, tissue sections were incubated with the second primary antibody and corresponding secondary antibodies. Tissue sections were washed three times in PBS containing 0.025% Triton X-100. Where indicated, tissue sections were counter-stained with 0.5 μg/ml DAPI for 10 min at room temperature, rinsed, and mounted in prolong gold antifade reagent (ThermoFisher, Waltham MA). Images were acquired using the Olympus IX81 inverted microscope at 10x, 20x, 40x or 100x objectives or Olympus 1X81 confocal microscope using 60x objective lens. The interaction of FDCs (CD35) with T_{FH} (PD-1) and B cells (CD20) was shown as colocalization sharing p27 antigen at their membranes. The formation of T_{FH} and B-cell stable complex was demonstrated in a similar manner.

Flow Cytometry

CLNs were harvested immediately after euthanasia; minced and treated with collagenase as described previously (35). Cells were then sieved through 40-μm nylon cell strainers with a 10-ml syringe plunger to make a cell suspension. Isolated cells were >90% viable as assessed by trypan blue exclusion. Cells were stained for surface antigens by incubating with fluorochrome-conjugated antibodies in staining buffer (PBS containing 2% fetal calf serum) for at least 30 minutes protected from light. The following fluorochrome-conjugated antibodies were used: CD20 (2H7), CD28 (CD28.2), CD35 (E11), CD4 (OKT-4), CD80 (2D10), CD95 (DX2), CXCR4 (12G5), ICOS (C398.4A) and PD-1 (EH12.2H7, Biolegend San Diego CA); CD21 (B-ly4), CD23 (M-L233), CD3 (SP34-2) and CD32 (8.26) (BD Biosciences, San Jose CA); and CXCR5 (MU5UBEE) (eBioscience, San Diego CA). FDCs were stained with Alexa Fluor® 488-conjugated SIVmac p27 antibody (55-2F12) or the isotype control IgG2b antibody without and with permeabilization in conjunction with the collagenase treatment. TFHs were also stained intracellularly with conjugated anti-p27 (55-2F12) or IgG2b and also BCL-6 (K112-91) or IgG1k (MOPC-21) (BD Biosciences). Collagenase (Sigma) treatment was performed with 1mg/ml at 37°C for 10 minutes and permeabilization was performed by utilizing FOXP3/Transcription factor staining buffer

(eBioscience, San Diego CA). Cells were fixed in intracellular fixation buffer for 30 minutes at room temperature in dark then washed twice in 1X permeabilization buffer before being resuspended in 1X buffer containing fluorochrome labeled antibody for detection of intracellular antigen. Cells were incubated for 45 minutes at room temperature in the dark, washed twice in 1X permeabilization buffer and resuspended in staining buffer for acquisition. LIVE/DEAD® Fixable Dead Cell Stain (Life Technologies, Carlsbad CA) was used to gate for the live cells. Samples were acquired on a BD LSRFortesa and analyzed using FlowJo software (Tree Star, Ashland OR).

RESULTS

Chronic infection with SIV results in varying levels of viral RNA loads in plasma, PBMCs and CLNs

To assess the level of SIV infection in rhesus macaques, SIV vRNA levels were measured at the time of necropsy in the plasma (up to 29 weeks after intravenous inoculation) in 11 SIVmac251 infected rhesus macaques. SIV vRNA was detected in plasma of all animals and ranged from 10^3–10^6 copies/mL (Fig. 1A). Thus, a robust chronic SIV infection was established in all 11 RMs that were infected. SIV vRNA was detected in plasma as early as one week after inoculation, peaked between 2–3 weeks, and remained at high set-point (10^3–10^6) levels until the end of the study (week 20–29) (Fig. 1C). Next, SIV vRNA levels were assessed in the PBMCs and CLNs to determine the relative difference in the magnitude in viral burden and infection between these two compartments. SIV vRNA levels expressed as copies/ng of RNA was found to be at significantly higher levels in the CLNs ($p = 0.004$) as compared to PBMCs (Fig. 1B). Typically, we expect to obtain approximately 50 μg of total RNA from 100mg of tissue samples and 8μg total RNA from 1×10^6 PBMCs or lymphoid cells.

B-cell follicles within CLNs trap high levels of SIV

Having established the presence of SIV vRNA in CLNs, we sought to determine whether SIV could be detected in BCFs within CLN. We also included 2 CLNs from SIV-naïve RMs for staining with hematoxylin-eosin to identify BCFs (Fig. 2A). The relative abundance of SIV burden was first determined on FDCs in the CLNs by immunohistochemistry for SIVp27 (Fig. 2A). Cells stained with SIVp27 gag protein were observed in CLNs obtained from chronically SIV-infected rhesus macaques, but not in the corresponding SIV-negative controls as seen by alkaline phosphatase based fast red (Fig. 2E–F) and DAB (Fig. 2G–H) chromogens. Therefore, chronic SIV infection of rhesus macaques resulted in substantial SIV acquisition by FDCs in the BCFs of CNS draining CLNs, in addition to accumulation shown in peripheral LNs by others (31, 32).

FDCs entrap substantial load of viral antigen within CLNs

To identify virus harboring cells within BCFs, IHC and IF analyses were performed to identify FDCs, B-cell aggregates, GCs and SIV by staining with CD35, CD20, PNA and SIVp27 antibodies, respectively. We observed CD20+ B-cell aggregates in BCFs (Fig. 3A). Then we looked for FDC architecture within BCFs. The signature reticular pattern of FDCs was clearly observed in the CLN BCFs by IF using confocal microscopy (Fig. 3B). CLNs

from SIV naïve rhesus macaques were populated with CD35 expressing FDCs (Fig. 3B) without any overlap with CD20+ B cells especially within the center of GCs (Fig. 3C). To confirm that FDCs harbored SIV, IF analysis was performed on CLN sections from SIV infected rhesus macaques for SIVp27, CD35 and DAPI (Fig. 3D). A significant proportion of FDCs within BCFs of the CLNs were observed positive for SIV p27 staining (Fig. 3D).

Having established the quantitative measure of SIV burden on FDCs in BCFs of CLN *in vivo*, further *ex vivo* studies were performed to better understand SIV acquisition by the FDCs. Cells were isolated from CLNs and characterized by surface and intracellular staining to determine FDC retention of SIV using antibodies to CD35, CD20 and SIVp27, along with appropriate isotype controls. Consistent with what has been demonstrated in peripheral LNs, we observed FDC frequencies to be 12.84±1.82% of total live cells to be $CD35^{+}/CD20^{-}$ FDCs within CLNs (Fig. 4A). These cells also expressed other FDCs markers such as CD21 and CD80 in good proportion 25.2% and 94.9%, respectively (Fig. 4A). In view of the ability of FDCs to trap antigen and retain it for an extended period of time, we assessed the frequency of FDCs carrying SIV mature gag protein p27 on the surface as well as within the cells. Without permeabilization, negligible presence of SIVp27 was observed on FDCs (Fig. 4B) while a considerable proportion of FDCs (24.74±6.03%, mean ± SEM) harbored intracellular SIVp27 (Fig. 4C), irrespective of collagenase treatment. These results suggest FDCs' entrapped SIV virions were primarily inside the cells as shown earlier in case of inguinal LNs (35).

Antigen harboring FDCs interact with B and T_{FH} cells in CLNs

A model of the interaction of FDCs with B and T_{FH} cells within the BCFs of CLN has been illustrated in Fig. 5A. Based on this model of cellular interactions in the BCFs, presence of cellular complexes would be indicative of FDC and B-cell interaction. FDCs trap and retain antigens in the form of specific antibody/complement-antigen immune complexes (ICs) allowing them to provide antigen to interact with B cell receptors (BCRs) on B cells. FDCs express adhesion molecules, FcR, and complement receptors 1 and 2 (CR1/CR2) on their cell surface. The ICs bind to FcRs and CRs (also known as CD35/CD21) on the FDC dendrites. To test the presence of these complexes, CLN sections were stained for B cells (CD20), FDCs (CD35) and SIV antigen (p27) respectively (Fig. 5B). We observed that FDCs that harbor SIV were in proximity to and in contact with B cells, giving an indication that cellular interactions and delivery of antigen to B cells was occurring in the BCF. The formation of cellular complexes was visible as clusters of cells consisting of FDCs and B cells in close proximity, as demonstrated by the co-localization of CD35, CD20 and SIVp27 within these cellular clusters. FDCs that express FcRs and complement receptors 1 & 2 (CD35/CD21) are capable of presenting immune complexes to B cell receptors in the BCF. Hence, it appears that not only do FDCs acquire SIV on their surface in a significant manner in the CLN, but these cells are able to form intimate cellular interactions with B-cells, which may drive antigen specific memory B-cell responses in CLNs. Additionally, the interactions between FDCs that harbor SIV (red) and T_{FH} (blue) cells was also examined, and as with B cells, FDCs form intimate interactions with T_{FH} within the BCFs (Fig. 5C). Our confocal imaging also demonstrated the presence of SIVp27 antigen in T_{FH} cells, which supports the notion of FDCs transferring SIV and infecting T_{FH} cells in the BCFs of CLNs (Fig. 5C).

This exchange of antigens is significant, considering the ability of T_{FH} cells to migrate from the BCFs and lymph nodes. We indeed observed higher proportion of infected T_{FH} cells on the periphery of BCFs of CLNs as compared to the center of BCFs, where the proportion of antigen loaded FDCs was higher (Supplementary Fig. 1).

Infected T_{FH} cells can interact with B cells in GC of CLNs

Finally, studies were performed to establish that SIV-infected T_{FHs} could interact with B cells in the BCF. T_{FH} cells express high levels of PD-1, which leads to decreased T_{FH} proliferation. In this regard, the qualitative nature of T_{FH} and B-cell interactions was determined by confocal microscopy, which demonstrated PD-1^{hi} expressing, infected T_{FH} cells surrounded by B cells (Fig. 5D). This interaction seems to be significant, considering the association between these complexes and hypergammaglobunemia in HIV patients. Thereafter, infected PD-1^{hi} TFH cells were shown by colocalization of PD-1 and SIVp27 (Fig. 6A). To confirm the quantitative nature of T_{FH} cell infection, flow cytometry was performed (Fig. 6B). Cells isolated from CLNs were examined for CD4, CD3, PD-1, CXCR5, BCL6, ICOS, CXCR4, CD95 and CD28 expression (Fig. 6B,C). $CD4^+/PD\text{-}1^+/CXCR5^+$ cells (Fig. 6B) were analyzed for intracellular expression of SIVp27 along with isotype controls (Fig. 6D lower panel). $CD4^+PD\text{-}1^+T_{FH}$ cells ranged from 0.65% to 3.49% of total CD4+ T cells isolated from CLNs (Fig. 6B, D upper panel). The phenotype of T_{FH} cells varied as a population with cells expressing ICOS (99.8%), CXCR4 (13.5%), CD28 (99.5%) and CD95 (100%). SIVp27 was detected in 73.1% to 90.9% of the total $CD4^+/PD\text{-}1^+/CXCR5^+$ positive T_{FH} cell population isolated from CLNs (Fig. 6D). Thus, not only do FDCs harbor and present SIV to B cells within BCF of CLNs, SIV infection is established in T_{FH} cells.

DISCUSSION

In this study, we attempted to establish that SIV trapped on the FDC network within CLNs may provide an additional viral reservoir, which would be distinct from the latent or persistent CNS reservoir that exists in perivascular macrophages, microglia and astrocytes. Although the presence of viral antigens was observed on FDCs in CLNs and in the sharing of antigen from FDCs to B cells and T_{FH} cells, future studies are required to more firmly establish the role of FDCs in CLNs as a viral reservoir and the relationship between this reservoir and viruses within the CNS. Furthermore, we need to investigate in greater detail the role of myeloid cell trafficking into the CNS and establish the significance of FDC accumulated virus in HIV infection. Monocyte trafficking into tissues is crucial to understand viral persistence during cART and its impact on HIV disease. These cells undergo continuous slow trafficking from blood to tissues and differentiate into macrophages and immature dendritic cells via afferent lymphatics. As such, they may contribute to establishment of cellular reservoirs that are unaffected by cART (42, 43).

A significant proportion of FDCs within CLNs were observed to harbor SIV, after establishment of primary infection. Indeed, SIV harboring FDCs were shown here to directly interact and co-localize with B and T_{FH} cells. This interaction is significant as it can lead to antigen-specific memory B-cell response and the infection of T_{FH} cells, respectively. Finally,

we also demonstrated that B-cells are in intimate contact with T_{FH} cells, which has been found to be associated with hypergammaglobulinemia, a means of immune response evasion by HIV (44). Based on these observations, we infer a novel role for CLN FDCs in viral entrapment and creation of a persistent SIV reservoir with potential importance to HIV neurological infections. Hence, our study highlights the role of FDCs in accumulation and transmission of HIV with implications for HIV egress from the CNS.

FDCs are known to act as an archive of infection and possess ability to indirectly infect nearby $CD4^+$ T_{FH} cells via an immune synapse involving B cells (34). FDCs are in direct contact with B cells and $T_{FHs.}$ It has been reported that human FDCs isolated from patients on cART retain infectious virus within a non-degradative cycling compartment. FDCs retain and recycle virus immune complexes, and as such only a fraction of the virus need be present on the FDC network and the remaining fraction may be retained in the endosomal compartment. This FDC retained virus is able to infect CD4+ T cells in *in vitro* experiments (35). These observations add further support to our studies and the potential impact of FDC associated virus in HIV disease.

Long lived reservoirs pose the most significant obstacle to a cure of HIV. While much has been gleamed from studies of CD4+ T cell reservoirs, less is known about other cellular or tissue reservoirs, including the CNS. A direct link between the CNS with CLNs via the meningeal lymphatic system has been demonstrated (12–17). “Glymphatics” refers to a tunnel of astrocytes (a subpopulation of glial cells) surrounding the blood vessels in the brain. They have been shown to be responsible for flow of brain interstitial fluid into cerebrospinal fluid (CSF) (17, 45). Interstitial fluid first drains from brain parenchyma to CSF via glymphatics (17, 45, 46). Subsequently, the flow of interstitial fluid into the CLNs involves dura mater lymphatic vessels. The connection of the CNS to the lymphatic system has been demonstrated in infectious disease models (i.e. cerebral malaria) (47) and in the maintenance of immune tolerance to self-antigens in the CNS (15). This route has also been proposed for the migration of HIV infected cells out of the brain (48). However, no studies have specifically looked at the role of CLNs in HIV infection so far. We hypothesized that cDCs upon entering into the CNS may encounter HIV virions or proteins released from productively infected cells (such as long-lived macrophages and microglia) or apoptotic bodies of short-lived perivascular macrophages. Thereafter, infiltrating into CSF and moving from cribriform plate to the lymphatic system of the nasal mucosa finally draining into deep CLNs.

To test our hypothesis, we first presented evidence for the accumulation of the virus in CLNs. Levels of viral RNA were shown to be significantly higher in CLNs than PBMCs of SIV infected rhesus macaques. Reports in the past have shown similar observations in peripheral lymph nodes (49, 50). The majority of SIV burden within CLNs was found to be contained in the BCFs on FDCs, which is in line with previous reports for peripheral lymph nodes (51). Given FDCs established role as an HIV-1/SIV reservoir (5, 30, 32, 34, 36, 37, 51), we determined that as high as 39% of the total FDCs in samples from CLNs harbored SIV (as measured by SIVp27 protein staining). This virus could either be bound on the surface of FDCs or within the cycling endosomes for extended periods of time (30, 35, 52). Subsequent interactions of these FDCs with BCF trafficking target cells might result in

infection of these cells and may also provide a route of virus egress out of the CLNs and into the CNS. Consistent with FDCs studied from other LNs, FDCs from CLNs of SIV-infected rhesus macaques are also a site for significant viral accumulation. HIV held on the surface of FDCs does not replicate or evolve; however, it retains the ability to infect cells that traffic nearby (36). Importantly, although FDCs themselves remain uninfected, they reside immediately adjacent to activated $CD4^+$ T and B cells within GCs and the long dendritic processes of FDCs interact directly with these adjacent lymphocytes. $CD4^+$ T-follicular helper (T_{FH}) cells are a specialized $CD4^+$ T-cell population in the BCF and play a seminal role in formation of the GC (53). Of note, FDCs can facilitate infection of $CD4^+$ T_{FH} cells (39, 54, 55).

In order to assess the cellular interactions of FDCs harboring SIV in BCFs of CLNs, we identified cellular complexes of FDCs with B cells in chronically SIV-infected CLNs using confocal microscopy. These interactions could lead to the development of SIV specific germinal center reactions and memory B-cell responses in CLNs, as well as potentially being a source of the hypergammaglobulinemia that is a hallmark of HIV/SIV infections. In addition to their capability to retain immune complexed antigen, FDCs have been shown to attract B cells and specific T cells into the BCFs to generate germinal center reactions (34, 56, 57). Consistent with what has been demonstrated in peripheral lymph nodes (44, 58) (59), we demonstrate that SIV harboring FDCs intimately interact with T_{FH} cells within BCFs and that a high frequency of T_{FH} are infected with SIV in CLNs. Since T_{FH}, and other CD4+ T cell subsets, are dynamic cells that migrate out of lymph nodes (60), the interactions between FDCs and T_{FH} in CLNs may be important in the context of understanding CNS infection.

The interaction between T_{FH} and B cells increases the turnover of B cells in the follicles of peripheral lymph nodes. This strong interaction between T_{FH} and B cells has been demonstrated in a number of studies (44, 58, 61–63). Furthermore, the expansion of T_{FH} cells in lymphoid tissues has been found to be associated with high titers of virus specific antibodies and heightened proliferation of B cells (61, 62, 64). In this regard, the formation of complexes with B and T_{FH} cells with antigen shared between the two could be demonstrated. A positive correlation between the T_{FH} cells in peripheral lymph nodes and hypergammaglobunemia has also been demonstrated by few studies, which contributes to production of large amounts of nonspecific antibodies and evasion of immune response by virus (44). Collectively, these interactions between FDCs, B and T_{FH} cells indicate that not only do FDCs act as carriers of SIV, but they also possess the capacity to infect the neighboring cells, an observation consistent with the characteristic features of viral reservoirs.

While our study highlights that HIV is trapped on FDCs, forms immune complexes with B cells and infects T_{FH} in CLNs, yet these observations are a prelude to determining that HIV trapped on FDCs in CLNs is a potential reservoir site. To unequivocally establish this viral reservoir site, one of the component of these studies will necessitate assessment and comparison of viral genotypes present in the periphery with virus in CNS perivascular macrophages, microglial cells, astrocytes and those associated with FDCs in CLNs in order to define the relationship of viruses between these compartments. These future studies will

be instrumental in establishing pathways of viral egress from the CNS into the periphery as well as determine the putative link between CNS infection and CLN reservoirs during the course of disease. Additional studies will also be essential to assess the phenotypic properties of viruses in the CLNs, which will confirm the pathogenicity of the virus in the CLNs and establish this site as a direct link with CNS infection. Overall, we have demonstrated that identification of additional reservoirs that may be involved in seeding additional genotypes back into the CNS.

Supplementary Material

Refer to Web version on PubMed Central for supplementary material.

Acknowledgments

Funding: These studies have been funded in part with NINDS R01 NS097147 to PJ and NIAID R01 AI113883; R21 AI114415; and R21 MH11345501 to SB.

References

1. Spudich S, Gisslen M, Hagberg L, Lee E, Liegler T, Brew B, Fuchs D, Tambussi G, Cinque P, Hecht FM, Price RW. Central nervous system immune activation characterizes primary human immunodeficiency virus 1 infection even in participants with minimal cerebrospinal fluid viral burden. J Infect Dis. 2011; 204:753–60. [PubMed: 21844301]
2. Avison MJ, Nath A, Greene-Avison R, Schmitt FA, Greenberg RN, Berger JR. Neuroimaging correlates of HIV-associated BBB compromise. J Neuroimmunol. 2004; 157:140–6. [PubMed: 15579291]
3. Matyszak MK, Perry VH. The potential role of dendritic cells in immune-mediated inflammatory diseases in the central nervous system. Neuroscience. 1996; 74:599–608. [PubMed: 8865208]
4. Pashenkov M, Huang YM, Kostulas V, Haglund M, Soderstrom M, Link H. Two subsets of dendritic cells are present in human cerebrospinal fluid. Brain. 2001; 124:480–92. [PubMed: 11222448]
5. Smith BA, Gartner S, Liu Y, Perelson AS, Stilianakis NI, Keele BF, Kerkering TM, Ferreira-Gonzalez A, Szakal AK, Tew JG, Burton GF. Persistence of infectious HIV on follicular dendritic cells. J Immunol. 2001; 166:690–6. [PubMed: 11123354]
6. Edén A, Price RW, Spudich S, Fuchs D, Hagberg L, Gisslén M. Immune activation of the central nervous system is still present after> 4 years of effective highly active antiretroviral therapy. Journal of Infectious Diseases. 2007; 196:1779–83. [PubMed: 18190258]
7. Zink MC, Brice AK, Kelly KM, Queen SE, Gama L, Li M, Adams RJ, Bartizal C, Varrone J, Rabi SA. Simian immunodeficiency virus-infected macaques treated with highly active antiretroviral therapy have reduced central nervous system viral replication and inflammation but persistence of viral DNA. Journal of Infectious Diseases. 2010; 202:161–70. [PubMed: 20497048]
8. Williams KC, Corey S, Westmoreland SV, Pauley D, Knight H, de Bakker C, Alvarez X, Lackner AA. Perivascular macrophages are the primary cell type productively infected by simian immunodeficiency virus in the brains of macaques: implications for the neuropathogenesis of AIDS. J Exp Med. 2001; 193:905–15. [PubMed: 11304551]
9. Fois AF, Brew BJ. The potential of the CNS as a reservoir for HIV-1 infection: implications for HIV eradication. Current HIV/AIDS Reports. 2015; 12:299–303. [PubMed: 25869939]
10. Churchill M, Nath A. Where does HIV hide? A focus on the central nervous system. Current opinion in HIV and AIDS. 2013; 8:165–9. [PubMed: 23429501]
11. Lamers SL, Gray RR, Salemi M, Huysentruyt LC, McGrath MS. HIV-1 phylogenetic analysis shows HIV-1 transits through the meninges to brain and peripheral tissues. Infection, Genetics and Evolution. 2011; 11:31–7.

12. Louveau A, Smirnov I, Keyes TJ, Eccles JD, Rouhani SJ, Peske JD, Derecki NC, Castle D, Mandell JW, Lee KS, Harris TH, Kipnis J. Structural and functional features of central nervous system lymphatic vessels. Nature. 2015; 523:337–41. [PubMed: 26030524]
13. Engelhardt B, Carare RO, Bechmann I, Flugel A, Laman JD, Weller RO. Vascular, glial, and lymphatic immune gateways of the central nervous system. Acta Neuropathol. 2016; 132:317–38. [PubMed: 27522506]
14. Louveau A, Harris TH, Kipnis J. Revisiting the Mechanisms of CNS Immune Privilege. Trends Immunol. 2015; 36:569–77. [PubMed: 26431936]
15. Mohammad MG, Tsai VW, Ruitenberg MJ, Hassanpour M, Li H, Hart PH, Breit SN, Sawchenko PE, Brown DA. Immune cell trafficking from the brain maintains CNS immune tolerance. J Clin Invest. 2014; 124:1228–41. [PubMed: 24569378]
16. Andres KH, von During M, Muszynski K, Schmidt RF. Nerve fibres and their terminals of the dura mater encephali of the rat. Anat Embryol (Berl). 1987; 175:289–301. [PubMed: 3826655]
17. Yang L, Kress BT, Weber HJ, Thiyagarajan M, Wang B, Deane R, Benveniste H, Iliff JJ, Nedergaard M. Evaluating glymphatic pathway function utilizing clinically relevant intrathecal infusion of CSF tracer. J Transl Med. 2013; 11:107. [PubMed: 23635358]
18. Aspelund A, Antila S, Proulx ST, Karlsen TV, Karaman S, Detmar M, Wiig H, Alitalo K. A dural lymphatic vascular system that drains brain interstitial fluid and macromolecules. J Exp Med. 2015; 212:991–9. [PubMed: 26077718]
19. van Zwam M, Huizinga R, Melief MJ, Wierenga-Wolf AF, van Meurs M, Voerman JS, Biber KP, Boddeke HW, Hopken UE, Meisel C, Meisel A, Bechmann I, Hintzen RQ, t Hart BA, Amor S, Laman JD, Boven LA. Brain antigens in functionally distinct antigen-presenting cell populations in cervical lymph nodes in MS and EAE. J Mol Med (Berl). 2009; 87:273–86. [PubMed: 19050840]
20. Ling C, Sandor M, Suresh M, Fabry Z. Traumatic injury and the presence of antigen differentially contribute to T-cell recruitment in the CNS. J Neurosci. 2006; 26:731–41. [PubMed: 16421293]
21. Cserr HF, Harling-Berg CJ, Knopf PM. Drainage of brain extracellular fluid into blood and deep cervical lymph and its immunological significance. Brain pathology. 1992; 2:269–76. [PubMed: 1341962]
22. Sagar D, Lamontagne A, Foss CA, Khan ZK, Pomper MG, Jain P. Dendritic cell CNS recruitment correlates with disease severity in EAE via CCL2 chemotaxis at the blood–brain barrier through paracellular transmigration and ERK activation. Journal of neuroinflammation. 2012; 9:1. [PubMed: 22212381]
23. Jain P, Coisne C, Enzmann G, Rottapel R, Engelhardt B. Alpha4beta1 integrin mediates the recruitment of immature dendritic cells across the blood-brain barrier during experimental autoimmune encephalomyelitis. J Immunol. 2010; 184:7196–206. [PubMed: 20483748]
24. Serafini B, Columba-Cabezas S, Di Rosa F, Aloisi F. Intracerebral recruitment and maturation of dendritic cells in the onset and progression of experimental autoimmune encephalomyelitis. Am J Pathol. 2000; 157:1991–2002. [PubMed: 11106572]
25. Zozulya AL, Ortler S, Lee J, Weidenfeller C, Sandor M, Wiendl H, Fabry Z. Intracerebral dendritic cells critically modulate encephalitogenic versus regulatory immune responses in the CNS. J Neurosci. 2009; 29:140–52. [PubMed: 19129392]
26. Hatterer E, Touret M, Belin MF, Honnorat J, Nataf S. Cerebrospinal fluid dendritic cells infiltrate the brain parenchyma and target the cervical lymph nodes under neuroinflammatory conditions. PLoS One. 2008; 3:e3321. [PubMed: 18830405]
27. Sagar D, Foss C, El Baz R, Pomper MG, Khan ZK, Jain P. Mechanisms of dendritic cell trafficking across the blood-brain barrier. J Neuroimmune Pharmacol. 2012; 7:74–94. [PubMed: 21822588]
28. Hollenbach R, Sagar D, Khan ZK, Callen S, Yao H, Shirazi J, Buch S, Jain P. Effect of morphine and SIV on dendritic cell trafficking into the central nervous system of rhesus macaques. Journal of neurovirology. 2014; 20:175–83. [PubMed: 23943466]
29. Kepler TB, Perelson AS. Cyclic re-entry of germinal center B cells and the efficiency of affinity maturation. Immunol Today. 1993; 14:412–5. [PubMed: 8397781]

30. Heesters BA, Chatterjee P, Kim YA, Gonzalez SF, Kuligowski MP, Kirchhausen T, Carroll MC. Endocytosis and recycling of immune complexes by follicular dendritic cells enhances B cell antigen binding and activation. Immunity. 2013; 38:1164–75. [PubMed: 23770227]
31. Grouard G, Durand I, Filgueira L, Banchereau J, Liu YJ. Dendritic cells capable of stimulating T cells in germinal centres. Nature. 1996; 384:364–7. [PubMed: 8934523]
32. Aguzzi A, Krautler NJ. Characterizing follicular dendritic cells: A progress report. Eur J Immunol. 2010; 40:2134–8. [PubMed: 20853499]
33. Deleage C, Wietgrefe SW, Del Prete G, Morcock DR, Hao XP, Piatak M Jr, Bess J, Anderson JL, Perkey KE, Reilly C, McCune JM, Haase AT, Lifson JD, Schacker TW, Estes JD. Defining HIV and SIV Reservoirs in Lymphoid Tissues. Pathog Immun. 2016; 1:68–106. [PubMed: 27430032]
34. Heesters BA, Myers RC, Carroll MC. Follicular dendritic cells: dynamic antigen libraries. Nat Rev Immunol. 2014; 14:495–504. [PubMed: 24948364]
35. Heesters BA, Lindqvist M, Vagefi PA, Scully EP, Schildberg FA, Altfeld M, Walker BD, Kaufmann DE, Carroll MC. Follicular Dendritic Cells Retain Infectious HIV in Cycling Endosomes. PLoS Pathog. 2015; 11:e1005285. [PubMed: 26623655]
36. Keele BF, Tazi L, Gartner S, Liu Y, Burgon TB, Estes JD, Thacker TC, Crandall KA, McArthur JC, Burton GF. Characterization of the follicular dendritic cell reservoir of human immunodeficiency virus type 1. J Virol. 2008; 82:5548–61. [PubMed: 18385252]
37. Banki Z, Kacani L, Rusert P, Pruenster M, Wilflingseder D, Falkensammer B, Stellbrink HJ, van Lunzen J, Trkola A, Dierich MP, Stoiber H. Complement dependent trapping of infectious HIV in human lymphoid tissues. AIDS. 2005; 19:481–6. [PubMed: 15764853]
38. Zhou X, Shapiro L, Fellingham G, Willardson BM, Burton GF. HIV replication in CD4+ T lymphocytes in the presence and absence of follicular dendritic cells: inhibition of replication mediated by α-1-antitrypsin through altered IκBα ubiquitination. The Journal of Immunology. 2011; 186:3148–55. [PubMed: 21263074]
39. Smith-Franklin BA, Keele BF, Tew JG, Gartner S, Szakal AK, Estes JD, Thacker TC, Burton GF. Follicular dendritic cells and the persistence of HIV infectivity: the role of antibodies and Fcgamma receptors. J Immunol. 2002; 168:2408–14. [PubMed: 11859132]
40. Rothenberger MK, Keele BF, Wietgrefe SW, Fletcher CV, Beilman GJ, Chipman JG, Khoruts A, Estes JD, Anderson J, Callisto SP, Schmidt TE, Thorkelson A, Reilly C, Perkey K, Reimann TG, Utay NS, Nganou Makamdop K, Stevenson M, Douek DC, Haase AT, Schacker TW. Large number of rebounding/founder HIV variants emerge from multifocal infection in lymphatic tissues after treatment interruption. Proc Natl Acad Sci U S A. 2015; 112:E1126–34. [PubMed: 25713386]
41. Byrareddy SN, Kallam B, Arthos J, Cicala C, Nawaz F, Hiatt J, Kersh EN, McNicholl JM, Hanson D, Reimann KA, Brameier M, Walter L, Rogers K, Mayne AE, Dunbar P, Villinger T, Little D, Parslow TG, Santangelo PJ, Villinger F, Fauci AS, Ansari AA. Targeting alpha4beta7 integrin reduces mucosal transmission of simian immunodeficiency virus and protects gut-associated lymphoid tissue from infection. Nat Med. 2014; 20:1397–400. [PubMed: 25419708]
42. Crowe S, Zhu T, Muller WA. The contribution of monocyte infection and trafficking to viral persistence, and maintenance of the viral reservoir in HIV infection. J Leukoc Biol. 2003; 74:635–41. [PubMed: 12960232]
43. Randolph GJ, Sanchez-Schmitz G, Liebman RM, Schakel K. The CD16(+) (FcgammaRIII(+)) subset of human monocytes preferentially becomes migratory dendritic cells in a model tissue setting. J Exp Med. 2002; 196:517–27. [PubMed: 12186843]
44. Lindqvist M, van Lunzen J, Soghoian DZ, Kuhl BD, Ranasinghe S, Kranias G, Flanders MD, Cutler S, Yudanin N, Muller MI, Davis I, Farber D, Hartjen P, Haag F, Alter G, Schulze zur Wiesch J, Streeck H. Expansion of HIV-specific T follicular helper cells in chronic HIV infection. J Clin Invest. 2012; 122:3271–80. [PubMed: 22922259]
45. Iliff JJ, Wang M, Liao Y, Plogg BA, Peng W, Gundersen GA, Benveniste H, Vates GE, Deane R, Goldman SA. A paravascular pathway facilitates CSF flow through the brain parenchyma and the clearance of interstitial solutes, including amyloid β. Science translational medicine. 2012; 4:147ra11–ra11.

46. Xie L, Kang H, Xu Q, Chen MJ, Liao Y, Thiyagarajan M, O'Donnell J, Christensen DJ, Nicholson C, Iliff JJ, Takano T, Deane R, Nedergaard M. Sleep drives metabolite clearance from the adult brain. Science. 2013; 342:373–7. [PubMed: 24136970]
47. Hoffmann A, Pfeil J, Alfonso J, Kurz FT, Sahm F, Heiland S, Monyer H, Bendszus M, Mueller AK, Helluy X, Pham M. Experimental Cerebral Malaria Spreads along the Rostral Migratory Stream. PLoS Pathog. 2016; 12:e1005470. [PubMed: 26964100]
48. Lamers SL, Rose R, Ndhlovu LC, Nolan DJ, Salemi M, Maidji E, Stoddart CA, McGrath MS. The meningeal lymphatic system: a route for HIV brain migration? J Neurovirol. 2016; 22:275–81. [PubMed: 26572785]
49. Jobe O, Ariyoshi K, Marchant A, Sabally S, Corrah T, Berry N, Jaffar S, Whittle H. Proviral load and immune function in blood and lymph node during HIV-1 and HIV-2 infection. Clin Exp Immunol. 1999; 116:474–8. [PubMed: 10361237]
50. Saksela K, Muchmore E, Girard M, Fultz P, Baltimore D. High viral load in lymph nodes and latent human immunodeficiency virus (HIV) in peripheral blood cells of HIV-1-infected chimpanzees. J Virol. 1993; 67:7423–7. [PubMed: 8230463]
51. Gerdes J, Flad H-D. Follicular dendritic cells and their role in HIV infection. Immunology today. 1992; 13:81–3. [PubMed: 1352451]
52. Tacchetti C, Favre A, Moresco L, Meszaros P, Luzzi P, Truini M, Rizzo F, Grossi CE, Ciccone E. HIV is trapped and masked in the cytoplasm of lymph node follicular dendritic cells. The American journal of pathology. 1997; 150:533. [PubMed: 9033269]
53. Fazilleau N, Mark L, McHeyzer-Williams LJ, McHeyzer-Williams MG. Follicular helper T cells: lineage and location. Immunity. 2009; 30:324–35. [PubMed: 19303387]
54. Estes JD, Thacker TC, Hampton DL, Kell SA, Keele BF, Palenske EA, Druey KM, Burton GF. Follicular dendritic cell regulation of CXCR4-mediated germinal center CD4 T cell migration. J Immunol. 2004; 173:6169–78. [PubMed: 15528354]
55. Thacker TC, Zhou X, Estes JD, Jiang Y, Keele BF, Elton TS, Burton GF. Follicular dendritic cells and human immunodeficiency virus type 1 transcription in CD4+ T cells. J Virol. 2009; 83:150–8. [PubMed: 18971284]
56. Ansel KM, Ngo VN, Hyman PL, Luther SA, Forster R, Sedgwick JD, Browning JL, Lipp M, Cyster JG. A chemokine-driven positive feedback loop organizes lymphoid follicles. Nature. 2000; 406:309–14. [PubMed: 10917533]
57. Caux C, Liu YJ, Banchereau J. Recent advances in the study of dendritic cells and follicular dendritic cells. Immunol Today. 1995; 16:2–4. [PubMed: 7880384]
58. Perreau M, Savoye A-L, De Crignis E, Corpataux J-M, Cubas R, Haddad EK, De Leval L, Graziosi C, Pantaleo G. Follicular helper T cells serve as the major CD4 T cell compartment for HIV-1 infection, replication, and production. The Journal of experimental medicine. 2013; 210:143–56. [PubMed: 23254284]
59. Haynes NM, Allen CD, Lesley R, Ansel KM, Killeen N, Cyster JG. Role of CXCR5 and CCR7 in follicular Th cell positioning and appearance of a programmed cell death gene-1high germinal center-associated subpopulation. J Immunol. 2007; 179:5099–108. [PubMed: 17911595]
60. Suan D, Nguyen A, Moran I, Bourne K, Hermes JR, Arshi M, Hampton HR, Tomura M, Miwa Y, Kelleher AD, Kaplan W, Deenick EK, Tangye SG, Brink R, Chtanova T, Phan TG. T follicular helper cells have distinct modes of migration and molecular signatures in naive and memory immune responses. Immunity. 2015; 42:704–18. [PubMed: 25840682]
61. Hong JJ, Amancha PK, Rogers K, Ansari AA, Villinger F. Spatial alterations between CD4+ T follicular helper, B, and CD8+ T cells during simian immunodeficiency virus infection: T/B cell homeostasis, activation, and potential mechanism for viral escape. The Journal of Immunology. 2012; 188:3247–56. [PubMed: 22387550]
62. Petrovas C, Yamamoto T, Gerner MY, Boswell KL, Wloka K, Smith EC, Ambrozak DR, Sandler NG, Timmer KJ, Sun X, Pan L, Poholek A, Rao SS, Brenchley JM, Alam SM, Tomaras GD, Roederer M, Douek DC, Seder RA, Germain RN, Haddad EK, Koup RA. CD4 T follicular helper cell dynamics during SIV infection. J Clin Invest. 2012; 122:3281–94. [PubMed: 22922258]

63. Fahey LM, Wilson EB, Elsaesser H, Fistonich CD, McGavern DB, Brooks DG. Viral persistence redirects CD4 T cell differentiation toward T follicular helper cells. J Exp Med. 2011; 208:987–99. [PubMed: 21536743]

64. Margolin DH, Saunders EF, Bronfin B, de Rosa N, Axthelm MK, Alvarez X, Letvin NL. High frequency of virus-specific B lymphocytes in germinal centers of simian-human immunodeficiency virus-infected rhesus monkeys. J Virol. 2002; 76:3965–73. [PubMed: 11907236]

A

Animal Number	Animal Name	Viral loads at necropsy (copies/ml)	Necropsy (weeks)
1	RTr14	3684	20
2	RQe14	199901	20
3	RMu14	27061	20
4	RVv14	37877	20
5	RIN14	49887	20
6	RDq14	9273440	20
7	RGS14	4522687	20
8	RQm11	28,249	27
9	RZe14	28,08832	26
10	RHy12	42906	27
11	RDv13	1923238	29

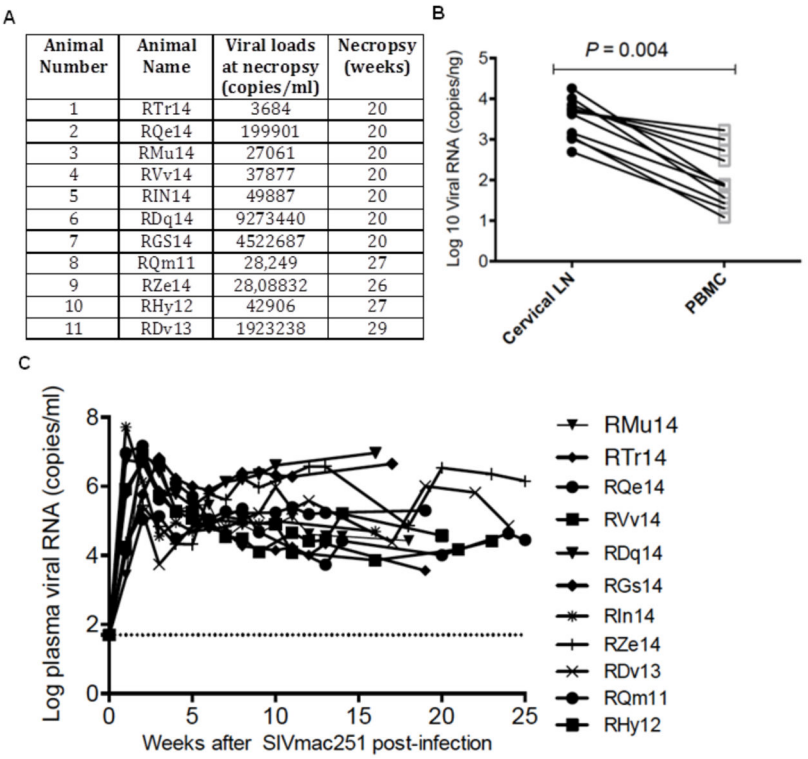

Fig. 1. SIV viral load at necropsy

(A) Viral load (Gag copies/ml) at time of necropsy. (B) Viral RNA (copies/ng) in CLNs and PBMCs derived from SIV-infected rhesus macaques during chronic infection. (C) Viral load over a period of 1–29 weeks after viral inoculation in plasma of SIV-infected rhesus macaques. The statistical significance was tested using two-tailed student t test. A p value <0.05 was considered statistically significant.

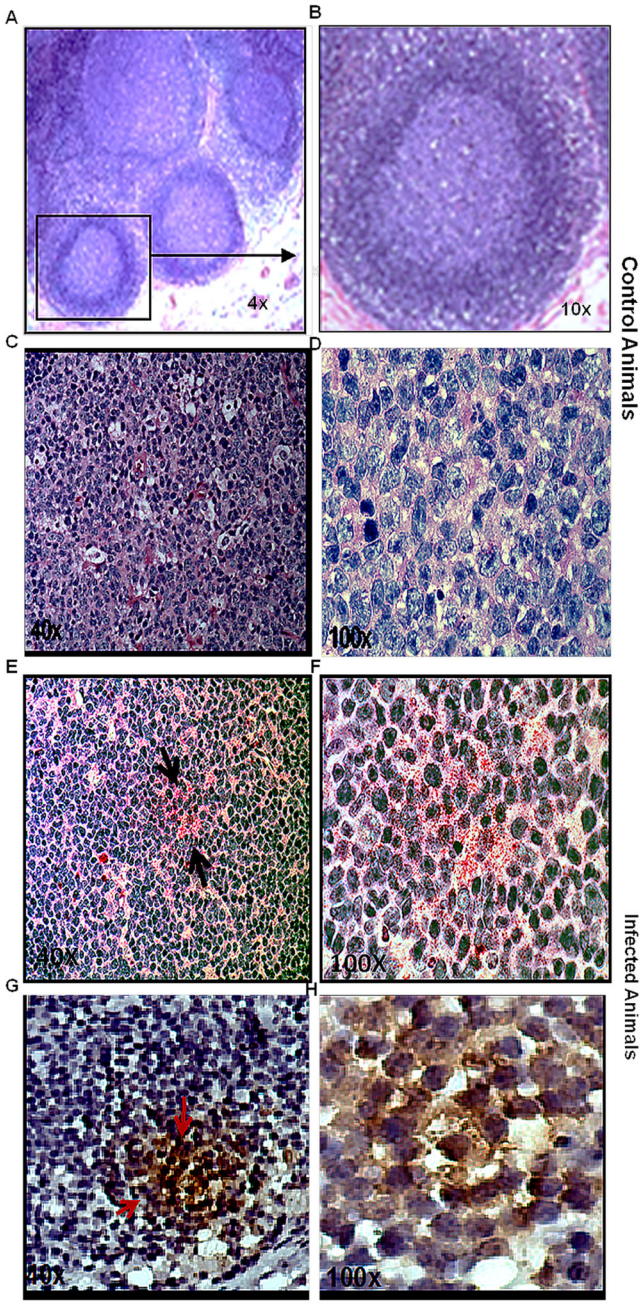

Fig. 2. SIV detection in B-cell follicles of CLNs

The CLN sections acquired from SIV naïve and infected rhesus macaque were stained using hematoxylin and eosin. Representative figure shows the GC architecture at 4X (A) and a magnified boxed image of one follicle at 10X (B). Immunohistochemistry on paraffin embedded CLN sections from SIV-naïve animal was done to detect p27 expressing cells. It showed no chromogen red signal confirming the absence of antigen as seen at 40X (C) and 100X (D) magnification. The sections from chronically infected animal showed positive chromogen red signals as indicated by arrows at both 40X (E) and 100X (F) magnification. Slides were also stained with DAB to further confirm SIV chromogen staining. Figures G

and H clearly show intense brown signals for DAB, which correspond to presence of p27 containing cells in the GC of chronically infected animals.

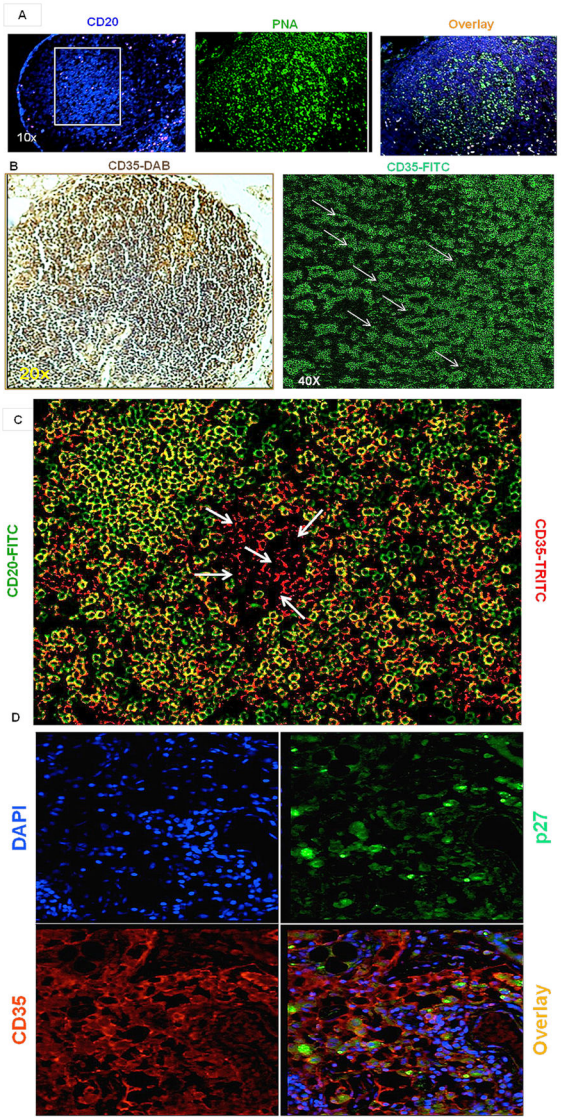

Fig. 3. Confirmation of SIV-bearing FDCs within CLNs of rhesus macaques

Immunohistochemistry and immunofluorescence on paraffin-embedded CLN sections from rhesus macaques was utilized to detect BCFs, CD35-positive FDCs and presence of viral p27 antigen. (A) Cells within the GCs from CLN of SIV-naive rhesus macaques were characterized by staining sections with anti-CD20 for B-cell aggregates (lymphoid follicles) and PNA for GCs. Representative images at 10x magnification indicate presence of CD20 (blue), PNA (green) and overlay of the two. (B) Representative image indicates the presence of CD35 immunofluorescence expressing cells, with a typical reticular arrangement marked with arrows and the blown image shows two such patterns after blow up of the image. (C) Distribution of CD20+CD35- B cells (green) and CD35+CD20- FDCs (red) within GCs of CLNs. The arrows show only FDCs distributed at the center of follicle. (D) Cells in the CLNs of SIV-infected rhesus macaques with chronic infection were characterized to identify the presence of p27 (green) (upper right) and CD35 (red) (bottom left) positive cells. Sections were stained with DAPI (upper left) to localize nuclei. Representative merged

image (bottom right) at 40x magnification indicate presence of p27 and CD35 positive cells within the CLNs.

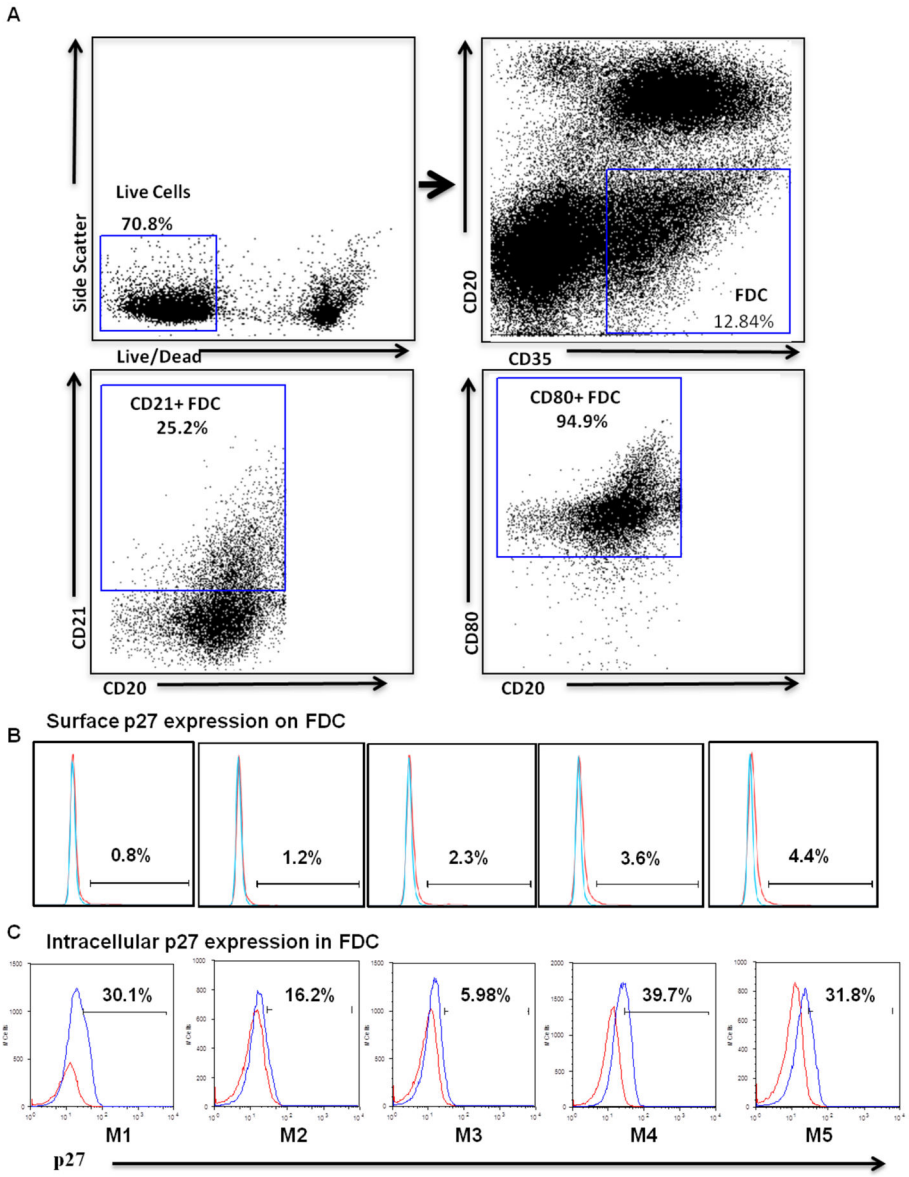

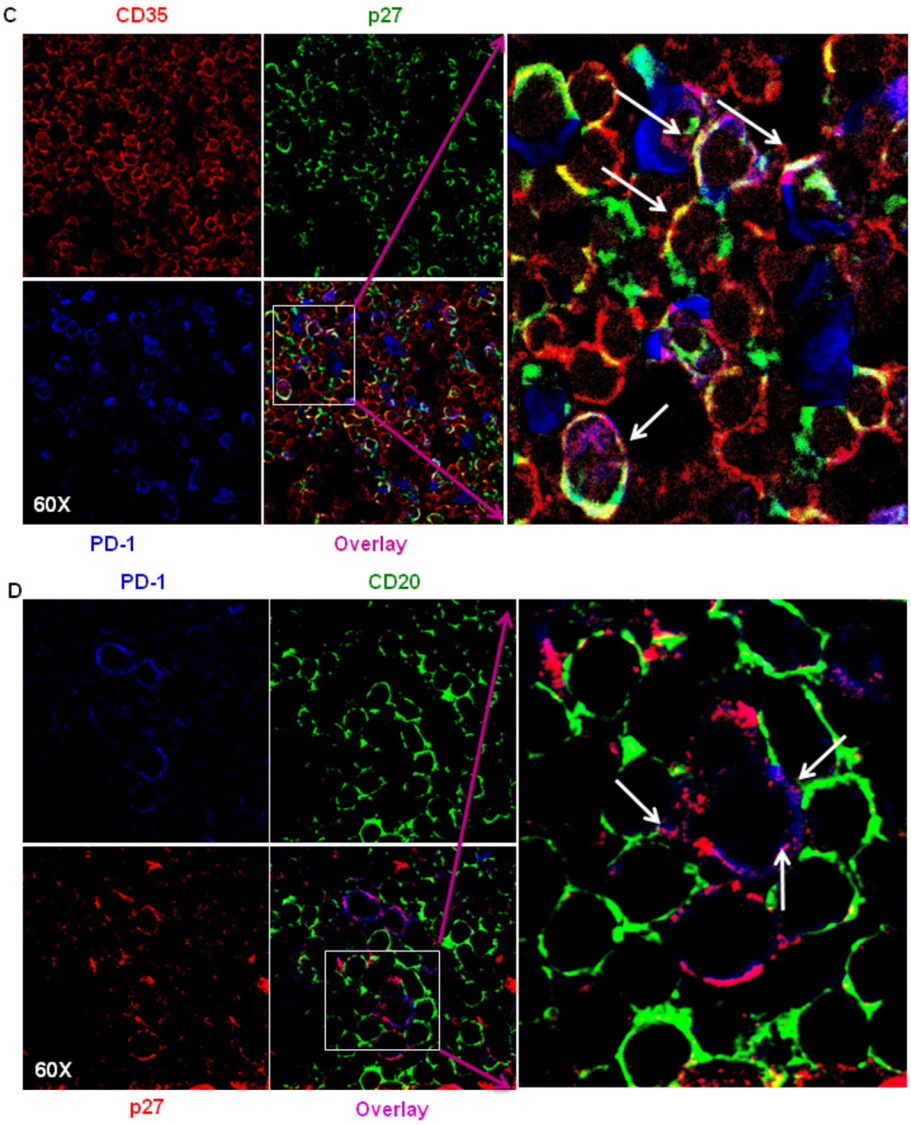

Fig. 4. FACS analysis of SIV-harboring FDCs within CLNs

Cells isolated from CLNs of chronically SIV-infected animals (week 29) (n = 5) were characterized by FACS analysis. Collagenase treated and untreated cells were surface stained for CD35 and CD20 markers. The cells which were not permeabilized were directly stained for p27 expression, whereas cells that were permeabilized (where indicated) were stained for intracellular SIV p27 expression. (A) Selection of FDCs by gating CD20-CD35+ cells (upper right) from live cell gate (upper left). $CD20^{-}/CD35^{+}$ cells were characterized for CD21 (lower right) and CD80 (lower right). FDC frequencies were found to be 12.84±1.82% of total live cells. These cells also expressed other FDCs markers such as CD21 and CD80 in good proportion 25.2% and 94.9%, respectively. Figure B shows SIV p27 surface staining on CD35+ CD20- FDCs in the histograms from 5 SIV infected rhesus macaques, while figure C shows intracellular SIV p27 expression in cells isolated from CLNs of chronically SIV-infected rhesus macaques. The surface expression of p27 was found to be negligible on FDCs. A considerable proportion of FDCs (24.74±6.03%, mean ±

SEM) harbored intracellular SIVp27. Blue and red line on the histograms corresponds to p27 and isotype control antibodies, respectively.

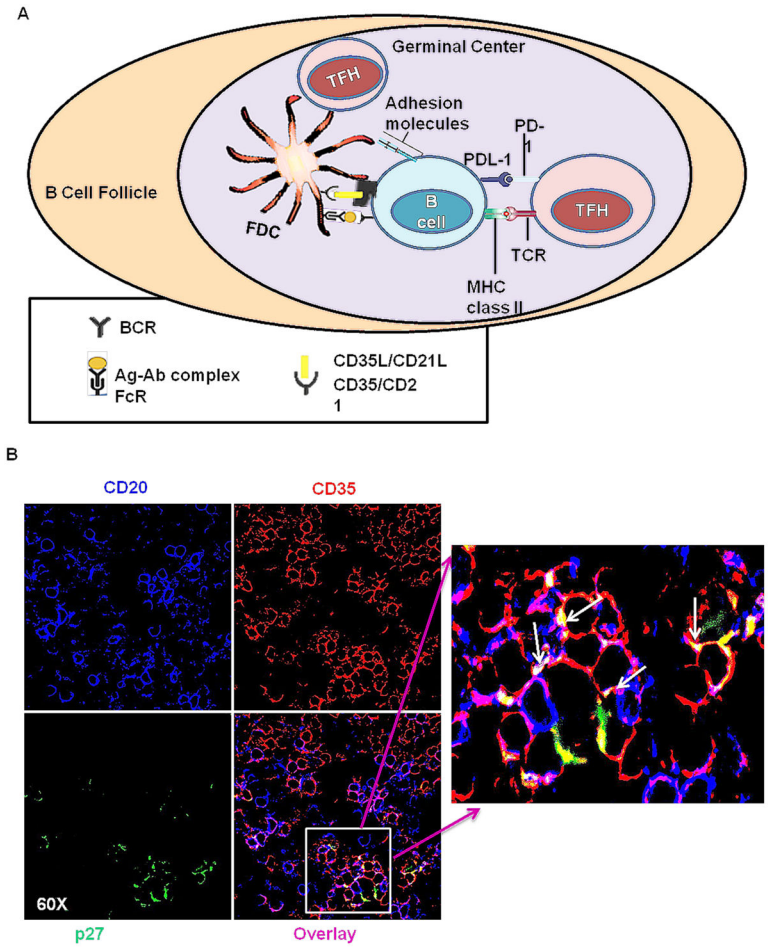

Fig. 5. Evidence of immune complexes and infection of T_{FH} cells within CLNs of chronically SIV-infected rhesus macaques

Model figure depicting the interaction of FDCs, B cells, and T_{FH} cells (A) within the GC of a secondary lymphoid organ. FDCs trap and retain antigens in the form of specific antibody-antigen immune complexes allowing them to provide antigen to interact with BCRs on GC B cells. FDCs express adhesion molecules, FcR, and complement receptors 1 and 2 (CR1/CR2) on their cell surface. The ICs bind to FcRs and CRs (also known as CD35/CD21) on the FDC dendrites. T_{FH} cells also express high levels of PD-1, which leads to decreased T_{FH} proliferation. The interaction of FDCs and B cells within the GC of CLNs (B). Cells from CLNs of chronically SIV-infected rhesus macaques were stained for CD20, CD35 and p27 expression. Representative profiles at 60x magnification indicate formation of immune-complexes, resulting from co-localization of CD20 (blue), p27 (green) and CD35 (red) signals. The arrows indicate the regions of colocalization. The antigen on the surface of FDCs could interact with B cells in the follicles of CLNs. Figure C shows transfer of viral p27 antigen (green) from $CD35^{+}$ FDCs (red) to PD-1^{hi} T_{FH} (blue) cells in GC of CLNs. The Figure shows antigen carrying FDCs in proximity to T_{FH} cells, with some of the T_{FH} cells being actually infected (colocalization of blue and green). The formation of the complex between CD20 (B cells) and (PD-1^{hi}) T_{FH} cells, with (p27) antigen shared at their

membranes was shown in figure D. This showed that FDCs can infect B cells and T_{FH} cells in the CLNs.

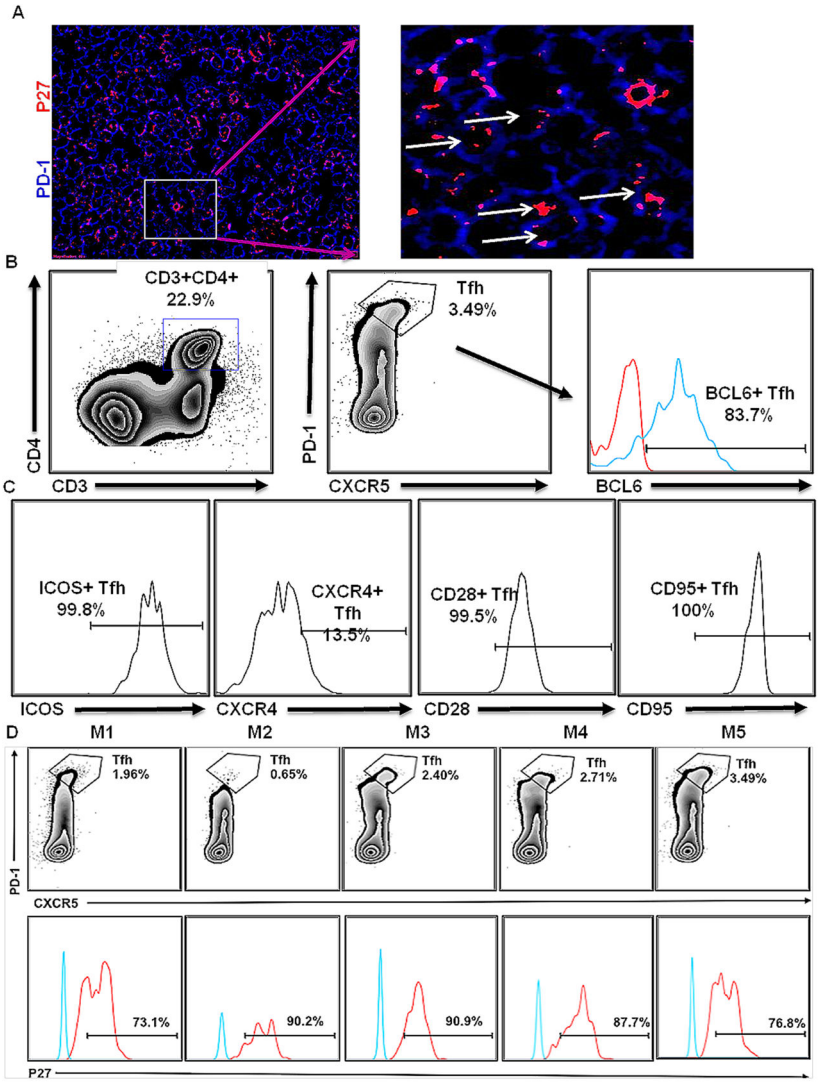

Fig. 6. Confirmation of SIV infection within TFHs of CLNs

The use of confocal microscopy showing the presence of p27 (red) in PD-1^{hi} TFH cells (blue) (A). The figure clearly shows intracellular antigen in T_{FH} cells as shown by arrows in magnified image. Cells isolated from CLNs of chronically SIV-infected rhesus macaques (week 29) (n = 5) were characterized by FACS analysis. $CD3^+CD4^+$ cells were gated to select $CXCR5^+PD\text{-}1^+$ T_{FH} cells (B). The phenotype of T_{FH} cells was established using staining for BCL6, ICOS, CXCR4, CD95 and CD28 expression (C). The percentages of T_{FH} cells in all rhesus macaque CLNs are shown in upper panel, while the percentages of T_{FH} cells showing intracellular p27 are shown in lower panel (D). Blue and red line on the histograms corresponds to BCL-6 or p27 antibody and isotype control antibodies, respectively.